RESEARCH ARTICLE

Aquatic versus terrestrial crab skeletal support: morphology, mechanics, molting and scaling

Jennifer R. A. Taylor*

ABSTRACT

The transition from aquatic to terrestrial environments places significant mechanical challenges on skeletal support systems. Crabs have made this transition multiple times and are the largest arthropods to inhabit both environments. Furthermore, they alternate between rigid and hydrostatic skeletons, making them an interesting system to examine mechanical adaptations in skeletal support systems. I hypothesized that terrestrial crabs have modified morphology to enhance mechanical stiffness and that rigid and hydrostatic skeletons scale differently from each other, with stronger allometric relationships on land. Using the aquatic blue crab, *Callinectes sapidus*, and the terrestrial blackback land crab, *Gecarcinus lateralis*, I measured and compared body mass, merus morphology (dimensions, cuticle thickness and the second moment of area *I*) and mechanics (flexural stiffness *EI*, elastic modulus *E*, critical stress and hydrostatic pressure) of rigid and hydrostatic stage crabs encompassing a range of sizes (*C. sapidus*: 1.5–133 g, $N \leq 24$; *G. lateralis*: 22–70 g, $N \leq 15$). The results revealed that rigid *G. lateralis* has similar morphology (limb length to diameter *L/D* and cuticle thickness to limb diameter *T/D* ratio) to *C. sapidus*, and the mechanics and most scaling relationships are the same. Hydrostatic land crabs differ from aquatic crabs by having different morphology (thinner cuticle), mechanics (greater internal pressures) and scaling relationship (cuticle thickness). These results suggest that the rigid crab body plan is inherently overbuilt and sufficient to deal with the greater gravitational loading that occurs on land, while mechanical adaptations are important for hydrostatically supported crabs. Compared with other arthropods and hydrostatic animals, crabs possess distinct strategies for adapting mechanically to life on land.

KEY WORDS: Crustacea, Exoskeleton, Hydrostatic skeleton, Mechanical properties, *Callinectes sapidus*, *Gecarcinus lateralis*

INTRODUCTION

The evolution of the rigid exoskeleton (i.e. cuticle) is considered a significant factor in the successful exploitation of land by arthropods (Bliss and Mantel, 1968; Jones, 1978; Kennedy, 1927; Raven, 1985; Wainwright, 1982). In addition to the major physiological advantage of providing a barrier to desiccation, exoskeletons yield biomechanical benefits in the form of protective armor and a strong support structure. In particular, an exoskeleton can achieve the same strength as an endoskeleton using less material, thereby reducing costs associated with material construction and skeletal mass (Currey, 1967). Yet, there are considerable biomechanical constraints for exoskeletons in terrestrial environments that may be mediated through different strategies and constrain body size or scale. Much of what is known about the functional morphology of exoskeletons on land comes from insects, but crabs are on average orders of magnitude larger, with *Birgus latro*, the largest terrestrial arthropod, reaching 4 kg in mass and a 75 cm leg span (Hamasaki et al., 2014; Hartnoll, 1988). Crabs, with their larger sizes, calcified exoskeleton and varied ecologies, may hold additional insights into the biomechanical constraints and adaptations of exoskeletons.

Crabs support the bulk of their bodies above the substrate with four pairs of walking legs (pereopods) that must also resist and transmit muscle contraction and ground reaction forces during locomotion. When stationary in still fluid conditions, crabs experience primarily gravitational forces, which are markedly reduced in water because of the counteracting effects of buoyancy. When crawling, aquatic crabs experience reduced ground reaction forces, but approximately 1000 times more drag than their terrestrial counterparts. The contrast in gravitational versus hydrodynamic forces is noticeable in semi-terrestrial crabs that adjust their body posture and walking kinematics when transitioning between these two media (Martinez et al., 1998). Despite drag being so significant in water, drag forces on the semi-terrestrial *Grapsus tenuicrustatus* were measured to be only about twice their submerged body weight when crawling at maximum velocity, and drag on an individual leg only 12% of whole body drag (Martinez, 2001). So while aquatic crabs are encumbered with hydrodynamic forces during locomotion, these forces are relatively small compared with the gravitational forces experienced on land. Walking leg segments (podomeres) of land crabs, therefore, are likely to experience greater forces during static and dynamic loading compared with those of their aquatic counterparts.

Crab podomeres are subject to bending, compression and torsion forces that must be resisted to avoid failure, which tends to occur by local buckling in exoskeletons (Currey, 1967; Hahn and LaBarbera, 1993; Parle et al., 2015). Flexural stiffness (*EI*) controls the deformations that occur during these common loading modes and helps determine the point at which local buckling occurs. Resistance to deformation and buckling can be improved by increasing the *EI* of the limb segment, where *E* is the elastic modulus, a material property, and *I* is the second moment of area, a structural property that describes the distribution of material away from the neutral plane. Animals with exoskeletons have multiple avenues for increasing limb stiffness and supporting greater gravitational loads on land, either by increasing the elastic modulus of the exoskeleton or by modifying appendage geometry, such as reducing the slenderness ratio (limb length to diameter, *L/D*) or increasing the cuticle thickness to limb diameter ratio (*T/D*).

As animals grow larger, both ontogenetically and evolutionarily, mechanical challenges become greater because body mass increases

Scripps Institution of Oceanography, Marine Biology Research Division, University of California, San Diego, La Jolla, CA 92093, USA.

*Author for correspondence (j3taylor@ucsd.edu)

J.R.A.T., 0000-0003-1799-8842

1

as the cube of the linear dimensions, but the strength of the skeleton increases as only the square of the linear dimensions (Alexander, 1971; Huxley, 1972; Schmidt-Nielsen, 1984; Swartz and Biewener, 1992). To remain functional as animals grow to larger sizes, modifications must be made in either morphology or mechanical properties, or both; otherwise, animals must reduce their performance (Biewener, 2003; Schmidt-Nielsen, 1984). In studies of terrestrial arthropods, several different strategies for dealing with problems of scale have been observed. Prange (1977) determined that the external dimensions of podomeres scale isometrically (in proportion to linear dimensions) for both a spider and a cockroach species, but cuticle thickness scales isometrically in the spider and allometrically (disproportionate to linear dimensions) in the cockroach. Locusts reveal yet another approach, with their jumping legs (metathoracic tibiae) growing allometrically and becoming more elongate (increasing L/D) (Katz and Gosline, 1992). While this would increase the risk of deformation, the mechanical stiffness also increases allometrically. Comparatively little is known about the strategies crabs use to cope with issues of mechanics and scale for exoskeletal support. Most studies on crustaceans focus on the relative growth of sexually dimorphic characters, such as the chelae and abdomen (for review, see Hartnoll, 1974, 1978, 1982; Teissier, 1960), and not skeletal support. Changes in exoskeleton mechanical properties or podomere shape may be needed to support the concomitant increases in mass and locomotor forces associated with growth, and crabs may use different strategies do deal with issues of scale in aquatic and terrestrial environments because of the dissimilar physical demands.

For most animals, growth is a continuous process, but for crabs that grow through molting, it is periodic and poses additional challenges. During molting, crabs shed the rigid cuticle and remain soft for several days until the new cuticle hardens, requiring that they temporarily support themselves with a hydrostatic skeleton (Taylor and Kier, 2003, 2006). Generally, animals possess only one skeletal support system throughout their adult life stage, so the intermittent use of a hydrostatic support mechanism presents unique mechanical constraints for crabs, including ones that may be sensitive to scale in ways that differ from those of rigid skeletons.

Animals with hydrostatic skeletons have a flexible body wall that encloses a volume of incompressible fluid, the pressure of which provides body turgor to support the animal and muscle antagonism to facilitate movement and locomotion (Chapman, 1958). The forces of muscle contraction transmit through the fluid, causing an increase in hydrostatic pressure. Resting and dynamic pressures are the primary sources of stress on the hydrostatic skeleton, which load the body wall in tension. The tensile stress on the body wall is proportional to the internal pressure and body or limb radius, but inversely proportional to body wall thickness, as described by Laplace's law:

$$\sigma_c = \frac{Pr}{t}, \qquad (1)$$

where σ_c is tensile stress in the circumferential direction, P is internal pressure, r is radius and t is body wall thickness. Hydrostatic skeletons tend to fail by puncture or tearing of the soft body wall, but also by local buckling, which may be prevented by high internal pressures (Currey, 1967; Kelly, 2007; Kier, 2012). Hydrostatic crabs have multiple ways to accommodate increases in tensile stress imposed on the cuticle, such as by modifying internal pressure, cuticle thickness to limb diameter ratio (T/D), or tensile properties of the cuticle.

Hydrostatic crabs are subject to additional difficulties in the terrestrial environment where the soft cuticle must support the body mass along with added water from postmolt inflation. A hydrostatic crab on land may have difficulty maintaining body shape because gravitational pressure becomes significant and places the animal at risk of becoming a 'pancake' (Currey, 1970). Gravitational pressure increases with increased height above the substrate and may explain why the largest worm, the giant gippsland earthworm *Megascolides australis*, can reach 380 g through increased length rather than diameter, which is limited to 20 mm (Van Praagh, 1992). The body depth of a crab can exceed this, reaching 33 mm in the ghost crab *Ocypode ceratophthalmus* (Haley, 1973), but surpassing this depth in larger species. Gravitational pressure is further increased when the body is held high above the substrate by the walking legs. If the hydrostatic legs of land crabs are unable to support the body above the substrate, then locomotion will be compromised. If crabs are unable to maintain their shape during molting, they will harden in a deformed state that impedes subsequent molts and leads to fatality (Bliss, 1979). Thus, constraints on the hydrostatic phase of crabs may predominate the rigid phase in influencing maximum body size on land.

Studies on the scaling of hydrostatic skeletons are limited to vermiform animals, particularly earthworms, and have shown that hydrostatic skeletons scale in different ways from rigid skeletons (Quillin, 1998). The scaling of body shape (length to diameter ratio) varies with ecotype, whereas body diameter and cuticle thickness tend to scale isometrically (Kurth and Kier, 2014, 2015; Lin et al., 2011; Quillin, 2000). In contrast, the mechanics, specifically internal hydrostatic pressure, remain constant across multiple orders of scale (Quillin, 1998, 1999). As defined by Laplace (Eqn 1), constant r/t and pressure means that stress on the body wall is independent of body size (Quillin, 1998). Hydrostatic crabs, with their more complex body plan and greater vertical height, may deal with the effects of scale in ways that differ from vermiform animals and even their rigid skeletal stage.

Crabs present a unique opportunity to compare the functional morphology of two distinct skeletal support systems in two contrasting environments, and ultimately gain insight into the biomechanical constraints and adaptations associated with molting and their transition to land. The goals of this study were to determine (1) how skeletal morphology and mechanics differ between aquatic and terrestrial crabs, (2) how the alternation between two distinct skeletons contributes to scale and (3) what effects the physical environment has on the scaling relationships of these two support mechanisms. It is hypothesized that terrestrial crabs have modified morphology to enhance flexural stiffness and that rigid and hydrostatic skeletons scale differently from each other, with stronger allometric relationships on land. These hypotheses were tested by evaluating the shape, mechanical properties and scaling relationships of a walking leg segment of the aquatic blue crab, *Callinectes sapidus*, and the terrestrial blackback land crab, *Gecarcinus lateralis*.

MATERIALS AND METHODS
Animals
Aquatic crabs
Blue crabs, *Callinectes sapidus* (Rathbun) (family Portunidae), were selected for this study because they are large, active and highly aquatic, with a hydrodynamic carapace and the fifth pair of pereopods paddle-shaped and specialized for swimming (Blake, 1985). Small to medium, male and female crabs (23–57 mm carapace width, 1.5–22 g) were collected from Masonboro Sound,

Wilmington, NC, USA, in 2004. Large 'peeler' crabs (within 2–3 days of molt) ranging from 63 to 112 mm carapace width (48–134 g) were obtained from a supplier in Wanchese, NC, USA, in 2004. Live crabs were maintained in individual seawater aquaria at a temperature of 19°C and a salinity of 15–20 ppt (Instant Ocean Artificial Seawater, Aquarium Systems Inc., Mentor, OH, USA). Peeler crabs were checked every 2 h for the onset of exuviation, while small and medium crabs were checked multiple times daily. For mechanical testing, seven large intermolt female crabs (109–127 mm carapace width) were purchased live from a local market in San Diego, CA, USA, in 2018 and euthanized in a −20°C freezer immediately prior to mechanical testing.

Terrestrial crabs
Blackback land crabs, *Gecarcinus lateralis* (Freminville) (family Gecarcinidae), were selected for this study because they are large and highly terrestrial, living in burrows and returning to water only to spawn. In addition, they molt without the buoyant support of water (Bliss and Mantel, 1968; Bliss et al., 1978; Hartnoll, 1988). Male and female land crabs (40–60 mm carapace width, 31–71 g) were collected from the Fajardo Reserve, Fajardo, Puerto Rico, in June 2003 and August 2004 and shipped to the University of North Carolina at Chapel Hill, NC, USA. Crabs were maintained in environmental chambers at 27°C on a 12 h light:12 h dark cycle. Humidifiers were used to keep room humidity within 60–90%. Individual crabs were housed in separate plastic containers with moistened sand and dishes of water. Containers were cleaned and crabs were fed carrots and lettuce twice a week and cat food once a week, with sand changed regularly.

Blackback land crabs do not have external changes in coloration indicative of molting like the blue crabs (Otwell, 1980), so the proximity of molt was estimated by monitoring the growth of limb regenerates (Bliss and Mantel, 1968; Skinner and Graham, 1972). To induce limb regeneration, one leg (pereopod 5), was removed from each crab by injecting a small amount of distilled water into the base of the leg.

For mechanical testing, eight specimens of *G. lateralis* (44–60 mm carapace width) were obtained in 2018 from a colony at Colorado State University and shipped to Scripps Institution of Oceanography on dry ice and promptly underwent mechanical testing.

Morphological measurements
Male and female crabs were combined for analyses to increase sample size and because dimorphism is only known to occur in the claws and abdomen (Haley, 1969, 1973; Herreid, 1967; Huxley, 1931). Only crabs that had undergone molting, appeared healthy and had all appendages intact were used. Measurements of the hydrostatic stage were taken immediately postmolt (1–3 h) whereas those of the rigid stage were taken 1–4 weeks postmolt. Time postmolt was calculated from the time exuviation was complete. Crab mass was measured using a balance prior to any limb removal. *Callinectes sapidus* was patted dry and weighed in air.

Pereopod 3 (i.e. the largest leg, often leading in sideways locomotion) was removed at the coxal–basal joint and the length, width and height of the merus segment were measured using digital vernier calipers. Measurements of merus length were taken at the midline on the anterior side of the segment, using landmarks for consistency. Merus height and width were both measured at the center of the segment. For *G. lateralis*, merus width was determined at the widest part, slightly ventral to the midline. All measurements were repeated 3 times, with standard error of measurements (s.e.m.) less than 0.01.

For cuticle thickness measurements, the measured merus was then fixed in either 10% formalin and seawater for *C. sapidus* or 10% formalin and deionized water for *G. lateralis*. All fixed samples were removed from formalin after several days and placed in 0.065 mol l^{-1} Sorensen's phosphate buffer for storage. The merus was cut transversely at the midline. Hard cuticle thickness was measured using a dissecting microscope with an ocular micrometer. Thirty measurements were taken around the circumference of the segment and separated into quadrants: anterior, posterior, dorsal and ventral. Measurements of mean cuticle thickness (*T*) were calculated in two ways to reflect bending in two axes: T_{height} is the mean of the dorsal and ventral sides of the merus, whereas T_{width} is the mean of the anterior and posterior sides.

The soft cuticle of hydrostatic stage animals was too thin to measure accurately using calipers and was therefore measured using laser scanning confocal microscopy. A rectangular section was cut from the middle of the anterior side of the merus and the hypodermis was carefully removed with a paintbrush. Cuticle samples were then immersed in poly-L-lysine for 20 min to aid the adhesion of fluorescent yellow green latex beads (L2153, Sigma-Aldrich, Inc., St Louis, MO, USA) to the inner and outer cuticle surfaces. Following immersion in poly-L-lysine, the samples were dipped in a suspension of the latex beads, placed on microscope slides and coverslipped. Thickness was measured from a Z-axis series in a confocal microscope as the distance between the beads on the inner and outer surfaces of the cuticle sample. For each cuticle sample, 10–30 measurements were taken and then averaged.

Second moment of area
The second moment of area, *I*, was calculated from digital microscope images of the merus cross-sections taken at the midline of the segment. The imaged cuticle was outlined and all non-cuticle material deleted, with the final image being converted to grayscale using Adobe Photoshop CS6 version 13.0. The second moment of area of the cuticle was calculated using the slice geometry function of BoneJ (Doube et al., 2010) in ImageJ (v. 1.51j8).

Flexural stiffness
Flexural stiffness, *EI*, for a beam in cantilever bending with an end-load is defined by:

$$3y = \frac{Fl^3}{EI}, \tag{2}$$

where *F* is the applied load, *l* is the length of the beam (between the support and applied load) and *y* is the deflection. Deflection of a beam is proportional to length cubed, so small increases in length result in large deformations, rendering long segments less resistant to bending. This classical beam theory equation assumes slender beams (*L/D*>10), where shear is negligible, with a constant cross-sectional shape. Crab meropodites have a lower *L/D* (Table 1), but are assumed to have negligible shear and a constant cross-sectional shape along the length of the merus, such that they can be characterized by classical beam theory. While this may induce some error, it is assumed to be acceptable for the comparative purposes of this study.

Pereopod 3 was separated at the coxal–basal joint using dissection scissors. The distal segments were then removed at the carpus, leaving the merus and adjacent joints intact. The basal–ischial–meral unit was placed in a block silicon mold, held upright and straight via mold prongs, and filled with epoxy (EpoxiCure, Buehler, Lake Bluff, IL, USA) such that 2–3 mm of the merus was

Table 1. Summary of measured variables for rigid and hydrostatic *Callinectes sapidus* and *Gecarcinus lateralis*

Stage	Variable	*Callinectes sapidus*		*Gecarcinus lateralis*	
		N	Adjusted mean	N	Adjusted mean
Rigid	Merus length (mm)	24	**20.06±1.18**	15	**24.01±2.30**
	Merus height (mm)	24	**6.85±0.70**	15	**7.98±0.70**
	Merus width (mm)	24	**3.21±0.20**	15	**4.24±0.31**
	Merus L/D_{height} (mm)	24	3.04±0.58	15	3.11±0.18
	Merus L/D_{width} (mm)	24	6.41±0.68	15	6.10±0.47
	T_{height} (mm)	24	**0.28±0.07**	15	**0.45±0.08**
	T_{width} (mm)	24	**0.16±0.04**	15	**0.26±0.05**
	T/D	24	0.05±0.03	15	0.07±0.02
	I (mm^4)	24	**7.81±2.89**	15	**19.85±4.39**
	E (MPa)	7	**10.45±10.80**	7	**2737±692**
	EI (N m^2)	7	0.004±0.002	8	0.006±0.003
	σ_{Cr} (MN m^{-2})	7	4.07±1.05	7	3.61±2.56
Hydrostatic	Cuticle thickness (mm)	10	**0.024±0.003**	9	**0.021±0.002**
	T/D	10	0.003±0.001	9	0.003±0.0003
	Baseline pressure (Pa)	12	**1193±366**	14	**12,996±8359**
	Peak pressure (Pa)	12	**606±274**	13	**3465±1303**

L, limb length; *D*, limb diameter, measured as height (D_{height}) or width (D_{width}); *T*, cuticle thickness calculated from the mean of the dorsal and ventral sides of the merus (T_{height}) or from the mean of the anterior and posterior sides of the merus (T_{width}); *I*, second moment of area; *E*, elastic modulus.
Adjusted means are size corrected to a standard body mass of 58 g and presented ±s.d. Values that are significantly different between species are in bold.

embedded in the epoxy. Samples were placed in an enclosed container and covered with a seawater-soaked paper towel to keep them hydrated while the epoxy cured overnight. Mechanical testing was performed the next morning after confirming specimens were securely embedded with no joint movement. Samples were kept hydrated throughout testing.

Merus segments were tested in cantilever bending by clamping the embedded ends into steel grips such that the merus extended horizontally and was bent along the dorsal–ventral axis. The load was applied perpendicular to the dorsal surface of the merus near the distal end (at a distance approximately 5% from the distal end). Tests were carried out in a universal mechanical tester (E1000, Instron, Norwood, MA, USA) equipped with a 50 N static load cell (model 2530-437, 0.5 kN maximum, 0.125 N resolution, Instron). Load was applied until a deflection of 10% of the length of the appendage at a rate of 20 mm min^{-1}, with force and deflection continuously recorded. A series of three tests were performed on each sample and averaged. Flexural stiffness was calculated for each test using Eqn 2 with the assumptions of uniform cross-sectional shape and no shear.

Bending strength
The embedded leg segments used in the flexural stiffness tests above were kept in a freezer (−20°C) for approximately 4 months prior to testing for bending strength. It is acknowledged that the storage process may affect the mechanical properties, but all specimens were stored in the same manner so that comparisons between the species may still be made. The segments showed no visible signs of deterioration and remained securely embedded. Mechanical testing of the meropodites was conducted in the same manner as for flexural stiffness (see above), but the test was run until failure. The maximum load at failure was recorded, with failure characterized as either buckling or fracture of the merus cuticle. After testing, each segment was examined under a stereomicroscope for damage. In addition, the critical stress, σ_{cr}, of each merus was calculated following Hahn and LaBarbera (1993) based on Roark and Young (1975):

$$\sigma_{cr} = \frac{rFL}{I}, \qquad (3)$$

where *r* is the radius in the plane of bending, *F* is the maximum force at failure, *L* is the span between the base of the merus (surface of the epoxy block) and the point where the force was applied, and *I* is the second moment of area.

Cuticle tensile stiffness
The contralateral pereopods were removed from the same crab specimens used for the flexural stiffness measurements, which had subsequently been kept in a freezer (−20°C) for approximately 4 months prior to testing. Rectangular samples of cuticle (approximately 4 mm wide and 15–20 mm long) were cut from the posterior merus surface and gently cleaned of soft tissue using a paintbrush. For tension tests, each end of the cuticle sample was sandwiched between two 19 mm×19 m square aluminium grips using cyanoacrylate adhesive to augment the attachment. The grips were then securely sandwiched between the steel tensile grips of a universal mechanical tester (E1000, Instron) equipped with a 50 N static load cell (model 2530-437, 0.5 kN maximum, 0.125 N resolution, Instron), so that the cuticle samples were stretched in the longitudinal direction. Tension tests were conducted at a rate of 5 mm min^{-1} until failure, with force and displacement continuously recorded.

The force and displacement data for each test were converted to stress and strain for analysis. Stress, σ, was calculated as engineering stress:

$$\sigma = \frac{F}{A}, \qquad (4)$$

where *F* is the instantaneous force applied and *A* is the initial cross-sectional area of the sample perpendicular to the applied force. For cross-sectional area, the width and thickness at the center of the specimen were measured using a digital caliper.

Strain, ε, was calculated as engineering strain:

$$\varepsilon = \frac{\Delta L}{L_0}, \qquad (5)$$

where ΔL is the change in length of the sample and L_0 is the initial sample length (measured as the distance between the grips after sample placement in the mechanical testing machine).

Stress–strain curves were generated for each cuticle sample. Those for *C. sapidus* were typically J-shaped, whereas those for *G. lateralis* were linear (Fig. S1). Young's modulus of elasticity (i.e. stiffness), *E*, was therefore estimated with a tangent modulus, measured as the slope of the stress–strain curve between 10% and 50% of the strain at failure.

Hydrostatic pressure

Internal baseline and peak pressure were extracted from data collected during previous experiments (Taylor and Kier, 2003, 2006). Individual crabs were placed in an experimental tank and restrained with Velcro straps to prevent movement. A 23-gauge needle with catheter connected to a pressure transducer (BLPR, World Precision Instruments, Sarasota, FL, USA) was inserted into the merus of the cheliped so that it recorded pressure in the hemocoelic space just beneath the arthrodial membrane near the merus–carpus joint. The pressure transducer was connected to a preamplifier and computer via an A/D card. Calibrations of the pressure transducer were made before and after each series of experiments. Pressure recordings were made at a rate of 65 Hz with data acquisition software (Dataq, Akron, OH, USA). Internal pressure was measured in 12 *C. sapidus* (mass: 74.7–152.7 g) and 14 *G. lateralis* (mass: 16.9–54.7 g).

Analysis

Each measured parameter was corrected for body size and allometry by adjusting to a standard body mass (herein referred to as adjusted mean). Adjusted means were then tested for normality and homogeneity before being compared between species using either two-tailed *t*-tests or Mann–Whitney with a Bonferroni adjusted $\alpha=0.048$. Summary data are presented as means±s.d. *N* refers to the number of individuals from each species tested. The size

range of *C. sapidus* encompassed smaller individuals than that of *G. lateralis*; therefore, to enable comparison over the same scale, the dataset for *C. sapidus* was truncated (only animals with body mass >20 g) for scaling analyses, though all data are included in the figures and used for comparison of adjusted means between species. Scaling relationships were also determined using the complete dataset for *C. sapidus* and are provided in Table S1.

Scaling relationships among all measured variables were determined with both ordinary least squares (OLS) and reduced major axis (RMA) regression on log-transformed data using the *lmodel2* package (http://CRAN.R-project.org/package=lmodel2) in R (3.0.2). Scaling relationships are described as power functions in the form of $y=aM^b$, or in the linear form of $\log y=\log a+b\log M$, where *y* is the variable of interest, *a* is the intercept, *b* is the scaling exponent, or slope, and *M* is body mass. The *lmodel2* package calculates slopes and intercepts, along with their 95% confidence intervals (CIs). RMA and OLS regressions were similar for some variables but different for others. Conclusions are based on RMA regressions because this method accounts for measurement error of both independent and dependent data (Lovett and Felder, 1989; McArdle, 1988; Rayner, 1985), but OLS regressions are also provided for comparison (Table S1). The 95% CIs were used to compare scaling exponents and intercepts between species and against predictions for isometry.

RESULTS
Rigid skeletons
Merus shape

The length of the merus relative to a standard body mass (adjusted mean) was greater for *G. lateralis* than *C. sapidus* (Table 1; Mann–Whitney, $U=33$, $N=24$, 15, $P<0.001$), which was not reflected in the overlapping 95% CIs for the intercepts in the

Table 2. Summary of regression values for rigid *C. sapidus* and *G. lateralis*

Species	N	Measurement	b_0	b	95% CI	Intercept	95% CI
C. sapidus	16	Carapace width	0.33	0.350	0.330, 0.372	1.290	1.248, 1.330
	16	Merus length	0.33	0.342	0.283, 0.413	0.692	0.551, 0.807
	16	Merus height	0.33	**0.246**	0.202, 0.300	0.427	0.321, 0.514
	16	Merus width	0.33	0.277	0.223, 0.345	0.024	−0.108, 0.131
	16	Merus L/D_{height}	0	**0.131**	0.089, 0.193	0.195	0.073, 0.277
	16	Merus L/D_{width}	0	**0.105**	0.066, 0.168	0.587	0.463, 0.665
	16	T_{height}	0.33	0.470	0.305, 0.726	−1.443	−1.944, −1.118
	16	T_{width}	0.33	0.461	0.302, 0.702	−1.660	−2.134, −1.349
	16	T/D	0	**0.370**	0.216, 0.634	−2.154	−2.673, −1.852
	16	*I*	1.33	**1.131***	0.780, 1.639	−1.074*	−2.072, −0.705
	7	*E*	0.33	**3.171***	1.233, 8.152	−4.767*	−14.69, −0.906
	7	*EI*	1.33	3.104	1.190, 8.093	0.079	−10.840, 4.267
	7	σ_{cr}	0.66	**−0.784***	−2.034, −0.302	3.982*	3.022, 6.473
G. lateralis	15	Carapace width	0.33	0.310	0.255, 0.377	1.189	1.082, 1.278
	15	Merus length	0.33	0.346	0.225, 0.531	0.768	0.609, 1.171
	15	Merus height	0.33	0.253	0.154, 0.414	0.454	0.194, 0.612
	15	Merus width	0.33	0.282	0.189, 0.420	0.129	−0.094, 0.278
	15	Merus L/D_{height}	0	**0.182**	0.113, 0.293	0.171	−0.008, 0.282
	15	Merus L/D_{width}	0	**0.170**	0.097, 0.298	0.468	0.262, 0.586
	15	T_{height}	0.33	0.415	0.245, 0.702	−1.083	−1.544, −0.810
	15	T_{width}	0.33	**0.557**	0.340, 0.912	−1.460	−2.032, −1.110
	15	T/D	0	**0.593**	0.340, 1.032	−2.230	−2.936, −1.823
	15	*I*	1.33	**0.770***	0.511, 1.159	−0.071*	−0.698, 0.345
	7	*E*	0.33	**−0.701***	−1.794, −0.274	4.663*	3.963, 6.457
	8	*EI*	1.33	1.630	0.727, 3.660	3.810	0.489, 5.290
	7	σ_{cr}	0.66	**1.821***	0.686, 4.836	−0.758*	−5.704, 1.104

Regression slopes, intercepts and confidence intervals were calculated using reduced major axis regression (RMA). b_0, predicted scaling exponent for isometry; *b*, RMA scaling exponent; CI, confidence interval; σ_{cr}, critical stress. Exponents significantly different from isometry are in bold. Asterisks indicate values that are significantly different between species.

|

regression analysis (Table 2). Merus length increased isometrically for both species, with scaling exponents no different from the isometric value of 0.33 (Fig. 1A, Table 2). The adjusted means for both merus height and width were also greater for *G. lateralis* (Table 1; merus height: Mann–Whitney, $U=43$, $N=24$, 15, $P<0.001$; merus width: *t*-test, $t=-12.7$, d.f.=37, $N=24$, 15, $P<0.001$), though the intercept 95% CIs overlapped. Merus height and width of both species scaled with predictions for isometry (Fig. 1B,C, Table 2).

The length to diameter ratios (*L/D*), or the spindliness of the merus segments, were the same for the two species, regardless of whether diameter was measured as height (Mann–Whitney, $U=116$, $N=16$, 15, $P=0.07$) or width (Mann–Whitney, $U=128$, $N=24$, 15, $P=0.14$) (Table 1). Merus length and diameter are both linear dimensions that scale isometrically ($b_0=0.33$) and therefore the ratio *L/D* should remain constant across size. Both *C. sapidus* and *G. lateralis* showed a slight positive allometry in these ratios (Table 2).

The merus of *C. sapidus* was elliptical in cross-section (Fig. 2A), with variation in cuticle thickness around the perimeter (one-way repeated measures ANOVA, $N=24$, $P<0.001$) (Fig. 2B). Mean cuticle thickness of the anterior (0.06±0.04 mm) and posterior (0.11±0.06 mm) sides significantly differed from each other and from the dorsal (0.14±0.08 mm) and ventral (0.16±0.09 mm) sides (Holm–Sidak, $N=24$, $P<0.001$), while the dorsal and ventral sides were the same (Holm–Sidak, $N=24$, $P=0.086$).

The merus of *G. lateralis* was triangular in cross-section, with a thick, flat ventral surface (Fig. 2A). Cuticle thickness varied around the perimeter (Friedman repeated measures ANOVA on ranks, $\chi^2=37.56$, $N=15$, $P<0.0001$) (Fig. 2C), with anterior (0.22±0.05 mm) and posterior (0.22±0.04 mm) sides the same (Tukey, $P<0.05$) and significantly thinner than the dorsal (0.45±0.08 mm) and ventral (0.35±0.09 mm) sides, which were the same (Tukey, $P<0.05$).

Cuticle thickness
Gecarcinus lateralis had a greater adjusted mean cuticle thickness along both axes than *C. sapidus* (Table 1; Mann–Whitney, $U=16$, 10, $N=24$, 15, $P<0.001$). T_{height} and T_{width} scaled similarly for the two species, with scaling exponents not significantly different from isometry based on the 95% CIs, except for *G. lateralis* T_{width} (Fig. 3A, Table 2).

The adjusted mean ratio of cuticle thickness to limb diameter (*T/D*, limb diameter equivalent to merus height) was greater for *G. lateralis* (Table 1; Mann–Whitney, $U=81$, $N=24$, 15, $P=0.004$), though this was not evident in the regression analysis intercepts (Table 2). *T/D* scaled similarly for the two species, with positive allometry (Fig. 3B, Table 2).

Mechanical properties
Gecarcinus lateralis had a significantly greater adjusted *I* than *C. sapidus* (Table 1; Mann–Whitney: $U=2.0$, $N=24$, 15, $P<0.001$). The intercept 95% CIs further indicate that *G. lateralis* had a greater *I* for a given size (Table 2). While the scaling exponents were not significantly different between species (Fig. 4A, Table 2), the 95% CIs of *C. sapidus* encompassed the isometric value of 1.33, whereas those of *G. lateralis* did not and indicate negative allometry (Table 2).

The adjusted Young's modulus, *E*, of *G. lateralis* was two orders of magnitude greater than that of *C. sapidus* (Table 1; Mann–Whitney: $U=0.0$, $N=7$, $P<0.001$), which was also evident in the difference between the regression intercepts (Table 2). The scaling exponent of *C. sapidus* was consistent with positive allometry, which was significantly different from the negative allometry observed for *G. lateralis* (Fig. 4B, Table 2).
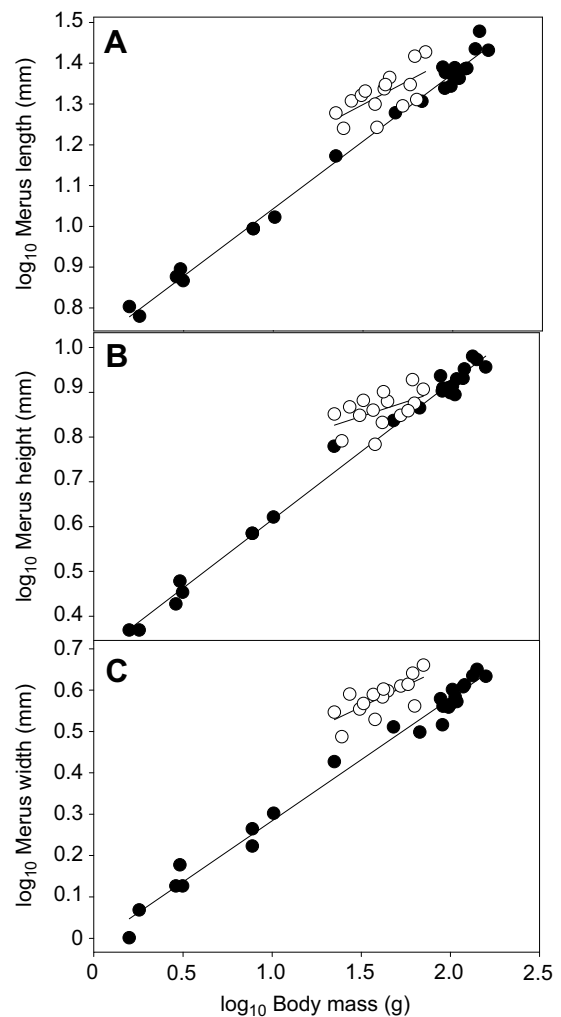

Fig. 1. Scaling of merus external dimensions. *Gecarcinus lateralis* (open circles) has a slightly larger merus length (A), width (B) and height (C) with respect to body mass than *Callinectes sapidus* (filled circles). All dimensions have a scaling exponent indistinguishable from isometry, except for *C. sapidus* merus height.

Adjusted flexural stiffness, *EI*, was the same for the two species (Table 1; *t*-test, d.f.=13, $t=-1.819$, $N=7$, 8, $P=0.09$), as also supported by the overlapping intercepts (Table 2). The large 95% CIs for both species did not distinguish the scaling exponents between species or from the prediction of isometry ($b_0=1.33$) (Fig. 5A, Table 2).

The adjusted critical stress, σ_{cr}, was the same for *C. sapidus* and *G. lateralis* (Table 1; *t*-test, d.f.=12, $t=-1.274$, $N=7$, $P=0.23$), although regression intercepts were different (Table 2). Both species had scaling exponents for critical stress that differed significantly from isometry and from each other (Fig. 5B, Table 2). For *C. sapidus*, critical stress scaled with negative allometry, while that for *G. lateralis* scaled with positive allometry (Table 2).

Hydrostatic skeletons
Adjusted cuticle thickness was greater for hydrostatic *C. sapidus* than for hydrostatic *G. lateralis* (Table 1; *t*-test, $t=2.212$, d.f.=17, $N=10$, 9, $P=0.041$), which was further supported by the non-overlapping intercept 95% CIs (Table 3). Cuticle thickness of both species scaled with negative allometry, and *G. lateralis* had a negative scaling exponent that was significantly different from that
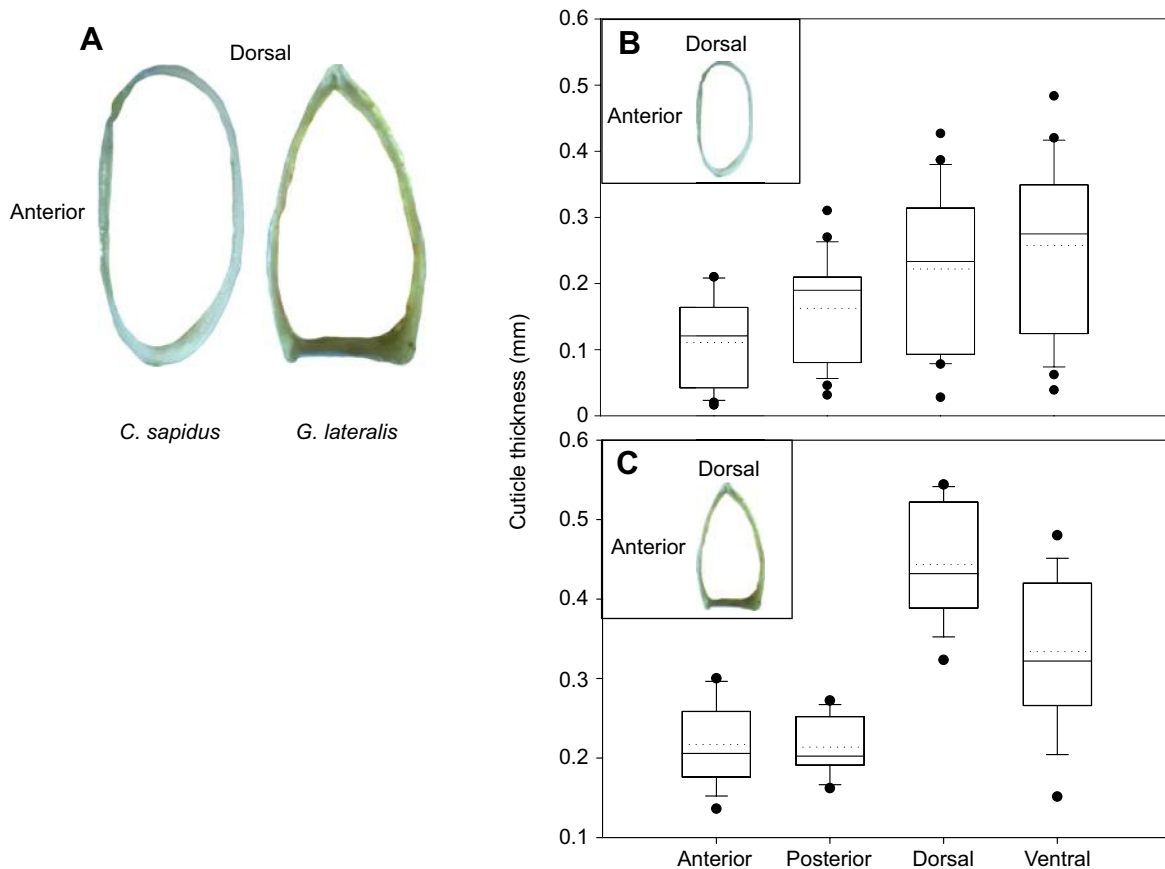
Fig. 2. Merus cross-sectional shape. (A) Microscope images reveal that the merus of *C. sapidus* is elliptical in cross-section whereas that of *G. lateralis* is triangular, with a flattened base. Mean cuticle thickness varies around the perimeter of the merus for both *C. sapidus* (B) and *G. lateralis* (C). All regions are significantly different in *C. sapidus*, whereas anterior and posterior regions are different from the dorsal and ventral regions in *G. lateralis*. Box boundaries: 25th and 75th percentile; error bars: 10th and 90th percentile; solid line: median; dotted line: mean.

of *C. sapidus* (Fig. 6A, Table 3). Despite differences in cuticle thickness, adjusted cuticle thickness to diameter ratio (*T*/*D*) was the same for the two species (Table 1; Mann–Whitney, *U*=44, *N*=10,9, *P*=0.97), scaling with similar exponents that reflect negative allometry (Fig. 6, Table 3).

Hydrostatic pressure

Adjusted baseline and peak pressure were significantly greater in *G. lateralis* than in *C. sapidus* (Table 1; Mann–Whitney, baseline: *U*=0.00, *N*=12, 14, *P*<0.001; peak: *U*=1.0, *N*=12, 13, *P*<0.001), though the intercept 95% CIs did not distinguish between them
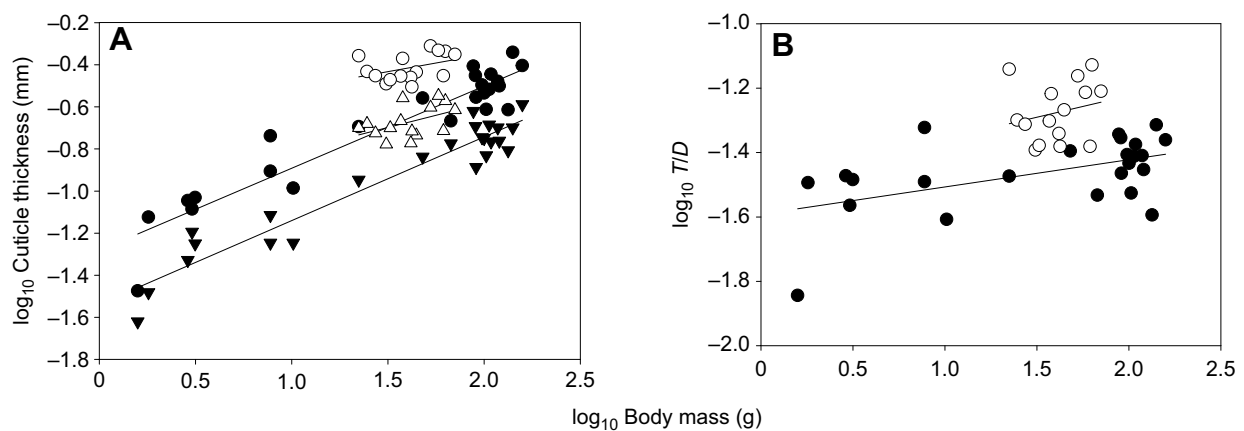
Fig. 3. Scaling of cuticle thickness in rigid crabs. (A) *Callinectes sapidus* (filled symbols) and *G. lateralis* (open symbols) have the same scaling exponents for cuticle thickness calculated from the mean of the dorsal and ventral sides of the merus (*T*$_{height}$, circles) and cuticle thickness calculated from the mean of the anterior and posterior sides of the merus (*T*$_{width}$, triangles). Aside from positive allometry in *T*$_{width}$ for *G. lateralis*, cuticle thickness scales isometrically. When corrected for body size, *G. lateralis* has a thicker cuticle. (B) Cuticle thickness to limb diameter ratio (*T*/*D*) scales with positive allometry for both species (*C. sapidus*: filled circles; *G. lateralis*: open circles), revealing that cuticle thickness increases at a greater rate than merus diameter.
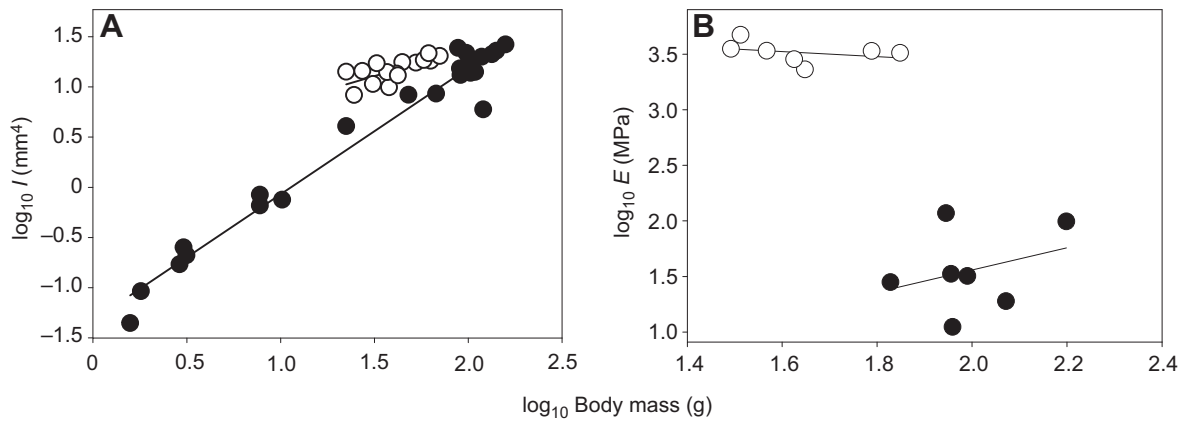
Fig. 4. Scaling of *I* and *E* for rigid crabs. (A) The second moment of area (*I*) for *C. sapidus* (filled circles) and that for *G. lateralis* (open circles) scale differently from one another. *I* scales with isometry for *C. sapidus* and negative allometry for *G. lateralis*. Size-adjusted *I* is greater for *G. lateralis*. (B) Cuticle stiffness, *E*, scales with positive allometry for *C. sapidus* and negative allometry for *G. lateralis*. Adjusted *E* is greater for *G. lateralis*.

(Table 3). Both measures of internal pressure scaled with positive allometry, with exponents not distinguishable between species (Fig. 7, Table 3).

Rigid versus hydrostatic
Scaling exponents of cuticle thickness and T/D differed between the rigid and hydrostatic states of both *C. sapidus* and *G. lateralis* (Table 2). Briefly, for *C. sapidus*, scaling of cuticle thickness of hydrostatic animals ($b=0.23$) differed from that of rigid animals ($b=0.47$), resulting in the scaling of T/D being negative in the former ($b=-0.15$) and positive in the latter ($b=0.37$; difference=0.52). For *G. lateralis*, the difference in cuticle thickness scaling between hydrostatic ($b=-0.17$) and rigid ($b=0.56$) animals was similar to that for *C. sapidus*, but resulted in almost twice the T/D difference between stages (hydrostatic: $b=-0.31$, rigid: $b=0.59$; difference=0.90).

DISCUSSION
The evolutionary transition from aquatic to terrestrial environments involves considerable shifts in the forces imposed on crab skeletons, yet adaptations in walking leg morphology and mechanics are not necessary to accommodate these different loading conditions. The crab exoskeleton appears to be overbuilt for their aquatic habitat and

sufficient to overcome the different physical challenges of the terrestrial environment. In contrast, the hydrostatic skeleton of crabs differs in morphology and mechanics between terrestrial and aquatic crabs, indicating that some modifications are necessary for molting crabs to function on land. While most of the scaling relationships of rigid exoskeletons are the same regardless of environment, those of the hydrostatic skeletons differ, with the effects of scale being more severe on land. Constraints for arthropod body size and locomotion on land are typically perceived as mechanical limitations of a rigid exoskeleton; however, those of the hydrostatic skeleton, albeit temporary, are likely more consequential.

Aquatic versus terrestrial exoskeletons
The walking leg meropodites of the land crab *G. lateralis* and the aquatic crab *C. sapidus* are similar in morphology (*L/D* and *T/D*) and mechanics (flexural stiffness and critical stress) despite these species living in physically contrasting environments. For crabs of moderate size, morphological modifications of the merus and enhanced stiffness are not necessary to accommodate the greater effects of gravity on land. This is possible if there are sufficiently large safety factors inherent in the crab body plan, which appears to be the case. For *C. sapidus* in this study, the mean estimated safety
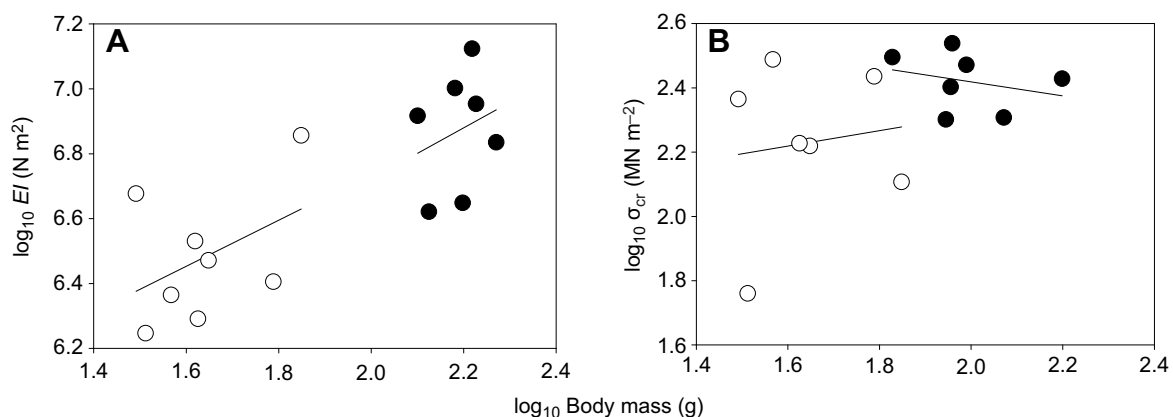
Fig. 5. Scaling of *EI* and σ$_{cr}$ for rigid crabs. (A) The flexural stiffness, *EI*, of both *C. sapidus* (filled circles) and *G. lateralis* (open circles) has scaling exponents not significantly different from isometry. Adjusted *EI* is the same for the two species. (B) Critical stress (σ$_{cr}$) scales with negative allometry for *C. sapidus* and positive allometry for *G. lateralis*. Adjusted critical stress is the same for the two species.

Table 3. Summary of regression values for hydrostatic *C. sapidus* and *G. lateralis*

Species	N	Variable	b_0	b	95% CI	Intercept	95% CI
C. sapidus	9	Carapace width	0.33	**0.351**	0.343, 0.360	1.297*	1.286, 1.308
	10	Cuticle thickness	0.33	**0.232***	0.149, 0.284	−2.033*	−2.112, −1.916
	10	*T/D*	0	**−0.145**	−0.242, −0.086	−1.936	−2.010, −1.811
	12	Pressure (baseline)	0	**0.981**	0.517, 1.860	1.328	−0.467, 2.275
	12	Pressure (peak)	0	**1.250**	0.650, 2.403	0.540	−1.815, 1.766
G. lateralis	10	Carapace width	0.33	0.350	0.290, 0.423	1.16*	1.049, 1.251
	9	Cuticle thickness	0.33	**−0.166***	−0.370, −0.075	−1.38*	−1.518, −1.074
	9	*T/D*	0	**−0.306**	−0.636, −0.147	−1.685	−1.924, −1.188
	14	Pressure (baseline)	0	**1.749**	0.989, 3.093	0.948	−0.992, 2.045
	13	Pressure (peak)	0	**1.416**	0.804, 2.494	1.004	−0.559, 1.892

Regression slopes, intercepts and confidence intervals were calculated using RMA. b_0, predicted scaling exponent for isometry; b, RMA scaling exponent. Exponents significantly different from isometry are in bold. Asterisks indicate values that are significantly different between species.

factor of a single merus under static loading (load at failure divided by submerged crab weight) is 88 (±30), which is comparable to the 50–70 estimated by Hahn and LaBarbera (1993). This large safety factor is more than adequate to accommodate the greater gravitational load a blue crab would experience on land. Indeed, large blue crabs are able to support themselves and crawl on land even though their submerged weight is less than 10% of their weight in air (Blake, 1985), but the safety factor drops tenfold. *Gecarcinus lateralis* may similarly be operating with lower safety factors rather than investing in morphological adaptations. Under static loading, the mean estimated safety factor for *G. lateralis* in this study is 61 (±34), which is not statistically different from that of *C. sapidus* in water (*t*-test: *t*=1.582, d.f.=12, *N*=7, *P*=0.14). It is perplexing that these two crab species have similar safety factors when they differ in mass, yet have the same critical stress. The answer may lie in the nature of merus failure, which, as discussed below, differs between the two species.

Though the relative merus dimensions are the same for *G. lateralis* and *C. sapidus*, the cross-sectional shape differs between the two species and it was hypothesized that these differences would be reflected in resistance to bending. The adjusted second moment of area, *I*, was significantly larger for the triangular merus of *G. lateralis* compared with the elliptical merus of *C. sapidus*, but this did not result in greater flexural stiffness, *EI*. This incongruity could stem from differences in cuticle stiffness, *E*, between species, but the adjusted tensile modulus was two orders of magnitude greater in *G. lateralis*. This should afford *G. lateralis* with greater flexural stiffness, yet the measured stiffness does not coincide with

the independently derived values of *E* and *I*. Such a mismatch may be attributed to oversimplification of merus morphology and applying simple beam theory equations to morphologically complex crab meropodites.

Interestingly, the two species have the same strategy of adding cuticle to the dorsal and ventral regions of the merus, which would enhance resistance in the vertical bending plane (Wainwright et al., 1976). In *C. sapidus*, local buckling has been observed proximally on the ventral surface of the merus (Hahn and LaBarbera, 1993), so this material reinforcement should serve to increase the critical buckling force. In this study, all seven of the meropodites tested experienced buckling, which is not surprising given that the merus radius relative to cuticle thickness (*r/t*) in the dorsal–ventral plane is approximately 12.0, slightly above the optimal 9.96 ratio to resist buckling (Taylor and Dirks, 2012). Here, buckling occurred longitudinally along the anterior surface (Fig. S2) rather than the ventral surface, as observed by Hahn and LaBarbera (1993). While this variation in buckling behavior might result from differences in sample preparation, testing or the fact that samples were frozen, it is also sensible that the surface with the thinnest cuticle would be the most susceptible to buckling. The dorsal and ventral parts of the merus, where cuticle is thicker, showed no visible buckling or fracture.

Neither the thicker cuticle nor the broad ventral surface of *G. lateralis* meropodites results in enhanced flexural stiffness or strength. Unlike *C. sapidus*, the meropodites of *G. lateralis* fracture rather than buckle. This makes sense given the lower *r/t* of 9.0, which would make the merus more susceptible to fracture (Taylor
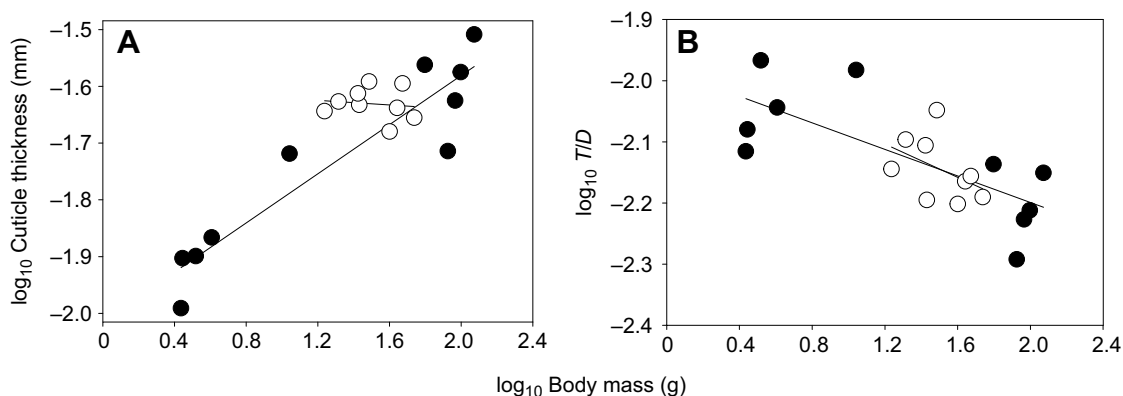
Fig. 6. Scaling of cuticle thickness in hydrostatic crabs. (A) Cuticle thickness scales with negative allometry for both *C. sapidus* (filled circles) and *G. lateralis* (open circles), with a significantly lower scaling exponent for the latter. This results in both species having negative allometry in *T/D* (B). *Gecarcinus lateralis* has a thinner cuticle but the same *T/D* as *C. sapidus* when adjusted for size.
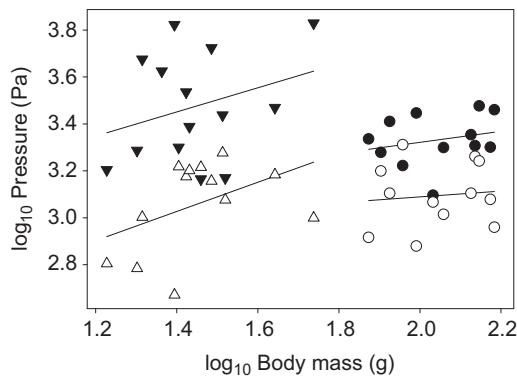
Fig. 7. Scaling of pressure in hydrostatic crabs. Baseline (open symbols) and peak (filled symbols) scale allometrically for both *C. sapidus* (circles) and *G. lateralis* (triangles). Scaling exponents for *G. lateralis* are greater, but not statistically distinguishable from those of *C. sapidus*. When adjusted for size, pressure is significantly greater for *G. lateralis*.

and Dirks, 2012). Cracks were heard in all samples during testing, but were variable in orientation and location, with some occurring on the sides, in the thicker ventral cuticle or dorsally at the point of load application. Thus, merus failure in *G. lateralis* appears to be governed by material strength and brittleness rather than geometry and buckling. It is unlikely that the triangular shape of the merus helps to increase the buckling strength of *G. lateralis*. Bee legs, which also have a triangular cross-section, were determined to have the same buckling strength as the circular legs of other insects, suggesting that this shape neither compromises nor enhances strength (Parle et al., 2015). A triangular cross-section, therefore, appears not to enhance stiffness or strength regardless of arthropod scale. For crabs, the triangular merus shape may have other functional significance, as it was observed to aid in sand transport during burrow digging by the ghost crab *Ocypode ceratophthalma* (Cott, 1929).

Scaling of rigid skeletons
The dimensions of the merus appear to change in similar ways as animals grow to larger sizes on land and in water. For both species, merus height and width grow more slowly than merus length. While the large CIs preclude statistically differentiating these scaling relationships from isometry, except for *C. sapidus* merus height, complementary patterns appear in the ratio of merus length to diameter (L/D), which increases disproportionately with body size for both species. The positive allometry of L/D indicates that the merus becomes spindlier in larger animals, which would make them prone to greater deflection during bending. Greater deformation would be expected to reduce locomotion efficiency, unless exoskeletal elasticity plays a role in pereopod extension, as in locusts (Katz and Gosline, 1992), or crabs increase merus stiffness, as described below.

Spindlier legs could also be generally advantageous for locomotion because having longer limbs increases stride length, which reduces the number of steps, and therefore cost, to move a certain distance (Schmidt-Nielsen, 1984; Taylor et al., 1970). It is somewhat surprising that the aquatic *C. sapidus* and the terrestrial *G. lateralis* have the same scaling relationships for merus shape given their different environments and locomotor proclivities. Several *Ocypode* land crabs, for example, exhibit negative allometry in merus length and increased curvature of the merus with size, essentially becoming more stout (Huxley, 1931; Sandon, 1937). Unlike *Ocypode* crabs, *G. lateralis* is more consistent with

C. sapidus and another land crab, *Cardisoma guanhumi*, as their merus grows isometrically in length and negatively allometric in width (Herreid, 1967). Merus shape appears to be less influenced by static and dynamic loading associated with basic crawling than by ecologically important specializations in locomotion. *Ocypode* crabs, for instance, are the fastest known crabs (Lochhead, 1961), reaching speeds of 4 m s^{-1} with the help of relatively long legs and a leaping gait (Burrows and Hoyle, 1973; Hafemann and Hubbard, 1969; Sandon, 1937). *Gecarcinus lateralis* and *Cardisoma guanhumi* are comparatively slower than *Ocypode*, which may explain the different merus scaling patterns. Increasingly spindlier meropodites with body size may be the norm for crabs, with departures from this shape only necessary for species adapted for specialized locomotion, such as high-speed running or tree climbing.

Merus T/D increased allometrically for both *C. sapidus* and *G. lateralis*, which would help provide additional stiffness to spindlier segments. The allometry of T/D is attributed to slight decreases in merus height with size, but also to increases in cuticle thickness. The scaling exponents for cuticle thickness are slightly higher than those predicted for isometry for both species, but cannot be distinguished from them by the large CIs, except for *G. lateralis* T_{width}. Isometric growth of cuticle thickness would help increase merus stiffness linearly with size, but also produce a heavier skeleton that could affect the buoyancy of aquatic crabs and be even more energetically costly to carry in terrestrial crabs. The cost of an increasingly heavier exoskeleton is a prevailing biomechanical argument for arthropod size limitation on land, so the disproportionately thicker cuticle for large *G. lateralis* is especially surprising. The cost of a heavier skeleton may be an acceptable tradeoff for greater desiccation, predator or impact resistance. Unfortunately, too few studies exist to distinguish adaptations and biomechanical constraints in aquatic and terrestrial crabs.

Isometric increases in both cuticle stiffness (E) and second moment of area (I) contribute to isometric increases in flexural stiffness (EI) of meropodites in *C. sapidus*. As the merus becomes spindlier in larger animals, however, the mechanical isometry is not sufficient to overcome the increased susceptibility to buckling, and critical stress decreases. For *G. lateralis*, the coupling of morphological and mechanical scaling is more complex. As meropodites become spindlier with increased size, both E and I scale with negative allometry, yet the resulting flexural stiffness is isometric and critical stress increases with size. A comparable mismatch in morphology and mechanics has been observed in the African desert locust, where flexural stiffness of the leg tibiae scales isometrically despite the segment becoming spindlier (Katz and Gosline, 1992, 1994). In the millipede *Nyssodesmus python*, cuticle thickness, I and EI all scale isometrically for both males and females, but cuticle stiffness and fracture strength only increase with size for females (Borrell, 2004). For the locust, the mismatch was attributed to allometric increases in cuticle stiffness, an explanation that cannot be extended to *G. lateralis*. Clearly, arthropods have developed different mechanisms for dealing with scale effects on the exoskeleton.

Aquatic versus terrestrial hydrostatic crabs
For hydrostatic animals, merus morphology (T/D) and internal fluid pressure determine the stress experienced by the cuticle. It was expected that the greater gravitational loading on land crabs would require one or both of these factors to be increased relative to their aquatic counterparts to maintain body shape and posture. This was

not the case for cuticle thickness, which was actually thinner in *G. lateralis*, nor *T/D*, which was the same for the two species; wall stress in land crabs is not relieved through modifications in merus morphology. Internal pressure, in contrast, was significantly greater in *G. lateralis* than in *C. sapidus*, supporting the hypothesis that larger pressures are indeed needed to support terrestrial hydrostats (Jones, 1978). Jones (1978) estimated that pressures of at least 1000–2000 Pa are necessary to support hydrostatic animals on land, which is achieved by both *C. sapidus* and *G. lateralis*. It is curious why *C. sapidus* should have such a high internal pressure when another aquatic hydrostatic animal, the sea anemone, has an average resting pressure of only 60 Pa (Batham and Pantin, 1950). Higher pressures result in greater body turgor, which would reduce deformation and thereby help crabs maintain their characteristic body shape.

The much higher internal baseline pressure of *G. lateralis* would place more stress on the cuticle, increasing the risk of tensile failure. The estimated baseline stress on the cuticle, using the adjusted means and Eqn 1, for *C. sapidus* was 0.17 MPa, which was significantly less than that of *G. lateralis* at 2.47 MPa. During muscle contraction, peak pressure increased the cuticle stress to 0.26 MPa and 3.13 MPa, respectively. Thus, the greater internal pressure combined with thinner cuticle in *G. lateralis* result in appreciably greater cuticle stress. The tensile strength of the soft cuticle, a measure of the ability to resist these pressure-induced stresses, has only been measured in *C. sapidus* (Taylor et al., 2007). With a tensile strength of 9.8 MPa, *C. sapidus* would have a safety factor of 38 during maximal muscle contraction. Rigid cuticle tensile strength of *G. lateralis* was measured in this study as 37±17 MPa, and if soft and rigid cuticles have the same tensile strength, as is the case for *C. sapidus*, then hydrostatic land crabs would be operating with a lower safety factor of 12. These high hydrostatic pressures put land crabs at a greater risk of tensile failure compared with aquatic crabs. In addition to tensile failure, hydrostats also risk impaired function due to local buckling. Pressurized cylinders are thought to be fairly resistant to local buckling because the pressure opposes compression during bending (Koehl et al., 2000). Avoiding buckling while hardening the exoskeleton postmolt is important if crabs are to maintain body shape. *Gecarcinus lateralis* may benefit from high pressures by having a reduced risk of buckling when molting on land under greater gravitational loading.

A unique aspect of hydrostatic support in crabs is that they must maintain their complex shape under pressure, without a rigid cuticle. Hydrostatic animals are predominantly vermiform shaped (Kier, 2012), because this is the most economical shape for containing fluids under pressure (Jones, 1978). Their cross-sectional shape tends to be circular under high internal pressure, but this can change when the animal is not maximally inflated (Clark and Cowey, 1958). For the hydrostatic merus to remain elliptical or triangular in cross-section, crabs may not be at maximal pressure and the cuticle must control the shape. Localized differences in cuticle tensile properties at the dorsal and ventral regions of the merus may prevent these regions from stretching. Variation in tensile properties could potentially stem from either thicker cuticle regions or localized differences in cuticle tanning rates, a process that occurs in the epicuticle prior to, during or immediately following ecdysis (Dennell, 1947; Krishnan, 1951; Travis, 1955; Williams et al., 2009). It is a greater challenge to maintain a triangular cross-sectional shape than an elliptical one, so *G. lateralis* may depart from *C. sapidus* in aspects of the cuticle tanning process.

Scaling of hydrostatic crabs

The hydrostatic skeleton of both *C. sapidus* and *G. lateralis* scaled differently from isometric predictions. As body mass increases, cuticle thickness increases at a slower rate, scaling with negative allometry. This results in a decreasing ratio of cuticle thickness to limb diameter (*T/D*) with size. According to Laplace, if pressure remains constant, then reduced cuticle thickness relative to diameter leads to increasingly greater tension in the cuticle for both species as they grow to a larger size. For *G. lateralis*, which has a negative scaling exponent, thickness of the outer cuticle layers (i.e. epicuticle and exocuticle) decreases slightly with body size, resulting in even greater cuticle tension as crabs grow. These scaling relationships contrast with the isometric scaling of body wall thickness in other hydrostats, such as caterpillars (Lin et al., 2011) and earthworms (Quillin, 1998). They also differ from the scaling relationships observed in the rigid state of these crabs, when the cuticle is fully formed and hardened.

Perhaps driving these different cuticle scaling relationships is the possibility that measurements of soft cuticle thickness may be biased toward smaller crabs that tend to molt more quickly and complete formation of the new cuticle sooner than larger crabs. This could contribute to the negative allometry observed, where smaller crabs have relatively thicker cuticles. All cuticle samples were taken from crabs within 1 h of ecdysis, when crabs were still completely soft, but cuticle layers were not examined. Small crabs may have formed more of the endocuticle layer by this time. It is interesting that this pattern was observed in both species and that *G. lateralis* had a negative scaling exponent. The molting process, including ecdysis, is generally slower for *G. lateralis* (Bliss, 1979; personal observation), so it would be surprising if the scaling of cuticle thickness was simply an artifact of measurement timing.

Based on decreasing *T/D*, larger crabs experience greater cuticle tension, which could be counteracted by a proportional decrease in internal pressure. This would deviate from isometric predictions of constant pressure, which occurs in earthworms over an order of magnitude size range (Keudel and Schrader, 1999; Kurth and Kier, 2014; Quillin, 1998). Instead, internal pressure increases with body size for both crab species, placing even more stress on the cuticle. To put this in perspective, as crabs grow from 10 g to 70 g in size, these scaling relationships would lead to a 7-fold increase in stress on the cuticle of *C. sapidus*, and a 65-fold increase for *G. lateralis*. The magnitude of these effects is clearly much greater for land crabs. Increased cuticle tension may require allometric scaling of the cuticle tensile properties. There have only been a few studies where the mechanical properties of soft cuticle were measured (Dendinger and Alterman, 1983; Dutil et al., 2000; Taylor et al., 2007), but none examined the effects of scale. Whereas Quillin (1998) excluded gravity from her scaling analysis of earthworms because it was considered insignificant for their low vertical height, it is relevant to land crabs. For land crabs, gravitational pressure presents a significant source of loading; not only are their bodies larger but also they are held above the substrate by the legs, increasing the vertical height even further. It is not clear why internal pressure scales allometrically for the aquatic *C. sapidus*, other than possibly to provide greater resistance to larger muscle contraction forces or being a requisite for maintaining the complex crab body shape.

For hydrostatic crabs, the effects of scale primarily manifest in reduced locomotor performance. It is known that molting negatively affects locomotion, as observed in the reduced jumping energy of grasshoppers (Gabriel, 1985; Queathem, 1991) and the slower, less forceful tail-flip escape response of lobsters (Cromarty et al., 1991). Reduced mobility is not likely to be due to molt-induced muscle

atrophy, which is limited to the large claws and facilitates their withdrawal at ecdysis (Ismail and Mykles, 1987; Mykles and Skinner, 1982, 1990). Large *C. sapidus* are noticeably slower immediately following molting than small individuals, which can swim without an appreciable loss in velocity (unpublished data). Locomotion is much more drastically affected in large *G. lateralis*, which are unable to hold their bodies off the substrate in the hydrostatic state and therefore move very slowly, using their large chelipeds to drag their bodies across the surface (personal observation). Small hydrostatic crabs, those less than 30 g, can support their bodies above the substrate with their legs and crawl relatively quickly (personal observation). For land crabs, there is a severe cost of scale in terms of locomotion. This is different from cylindrical earthworms, where burrowing and crawling are unaffected by increases in size (Quillin, 1999, 2000), a reflection of the challenge for hydrostatic support in the crab body plan. In general, locomotion in terrestrial hydrostatic animals, such as caterpillars and dipteran larvae, is many times more costly than that of arthropods of similar size with rigid exoskeletons (Berrigan and Lighton, 1993; Casey, 1991). For crabs, this high cost of locomotion in the hydrostatic phase increases with body size and cannot be overcome by adequate mechanical scaling strategies.

Conclusions

Crabs have many adaptations to life on land that reflect the physical, chemical and biological challenges of the terrestrial environment (Bliss and Mantel, 1968), yet they do not appear to require biomechanical adaptations of exoskeletal support. Comparison of the morphology and mechanics of walking leg meropodites from a highly aquatic species and a highly terrestrial species of crabs revealed no significant differences between them. In contrast, the hydrostatic skeleton used during molting differs between the two species, with higher internal pressure, higher stress and a lower cuticle thickness scaling exponent for land crabs. In the hydrostatic phase, both species experience significant decreases in locomotor performance as they grow to larger sizes, with scale effects being more dramatic in the terrestrial crabs.

The alternating use of two different skeletal support mechanisms presents additional complications for understanding how body size relates to skeletal morphology and function. Rigid and hydrostatic skeletons function by different mechanisms and are affected by scale in different ways. Thus, the two skeletons influence crab growth independently. In order to grow to a larger size, crabs must first successfully undergo ecdysis. If the hydrostatic animal cannot support its own weight and shape, severe deformations may occur that will compromise the hardened skeleton. Thus, the hydrostatic stage may present the more limiting stage, as suggested by Kennedy (1927) for why insects are limited to small size. Whether or not this is the case, the hydrostatic skeleton used by crabs during molting should be recognized as a biomechanical feature of significant importance in the growth to maximum size of crabs and their successful transition to land.

Supplementary information
Supplementary information available online at
http://jeb.biologists.org/lookup/doi/10.1242/jeb.185421.supplemental

References
Alexander, R. M. (1971). *Size and Shape*. London, UK: Edward Arnold.

Batham, E. J. and Pantin, C. F. A. (1950). Muscular and hydrostatic action in the sea-anemone *Metridium senile* (L.). *J. Exp. Biol.* **27**, 264-289.

Berrigan, D. B. and Lighton, J. R. B. (1993). Bioenergetic and kinematic consequences of limblessness in larval diptera. *J. Exp. Biol.* **179**, 245-259.

Biewener, A. A. (2003). *Animal Locomotion*. Oxford: Oxford Univ. Press.

Blake, R. W. (1985). Crab carapace hydrodynamics. *J. Zool.* **207**, 407-423.

Bliss, D. E. (1979). From sea to tree: saga of a land crab. *Am. Zool.* **19**, 385-410.

Bliss, D. E. and Mantel, L. H. (1968). Adaptations of crustaceans to land: a summary and analysis of new findings. *Am. Zool.* **8**, 673-685.

Bliss, D. E., Van Montfrans, J., Van Montfrans, M. and Boyer, J. R. (1978). Behavior and growth of the land crab *Gecarcinus lateralis* (Fréminville) in Southern Florida. *Bull. Am. Mus. Nat. Hist.* **160**, 115-152.

Borrell, B. J. (2004). Mechanical properties of calcified exoskeleton from the neotropical millipede, *Nyssodesmus python. J. Insect Physiol.* **50**, 1121-1126.

Burrows, M. and Hoyle, G. (1973). The mechanism of rapid running in the ghost crab, *Ocypode ceratophthalma. J. Exp. Biol.* **58**, 327-349.

Casey, T. M. (1991). Energetics of caterpillar locomotion: biomechanical constraints of a hydraulic skeleton. *Science* **252**, 112-114.

Chapman, G. (1958). The hydrostatic skeleton in the invertebrates. *Biol. Rev.* **33**, 338-371.

Clark, R. B. and Cowey, J. B. (1958). Factors controlling the change of shape of certain nemertean and turbellarian worms. *J. Exp. Biol.* **35**, 731-748.

Cott, H. (1929). Observations on the natural history of the racing-crab. *Ocypode ceratophthalmus. Proc. Zool. Soc. Lond.* **4**, 755-765.

Cromarty, S. I., Cobb, J. S. and Kass-Simon, G. (1991). Behavioral analysis of the escape response in the juvenile lobster *Homarus americanus* over the molt cycle. *J. Exp. Biol.* **158**, 565-581.

Currey, J. D. (1967). The failure of exoskeletons and endoskeletons. *J. Morphol.* **123**, 1-16.

Currey, J. D. (1970). *Animal Skeletons*. New York: St. Martin's Press.

Dendinger, J. E. and Alterman, A. (1983). Mechanical properties in relation to chemical constituents of postmolt cuticle of the blue crab, *Callinectes sapidus. Comp. Biochem. Physiol. A* **75**, 421-424.

Dennell, R. (1947). The occurrence and significance of phenolic hardening in the newly formed cuticle of Crustacea. *Proc. R. Soc. Lond. B.* **134**, 485-503.

Doube, M., Kłosowski, M. M., Arganda-Carreras, I., Cordeliéres, F., Dougherty, R. P., Jackson, J. S., Schmid, B., Hutchinson, J. R. and Shefelbine, S. J. (2010). BoneJ: free and extensible bone image analysis in ImageJ. *Bone* **47**, 1076-1079.

Dutil, J.-D., Rollet, C., Bouchard, R. and Claxton, W. T. (2000). Shell strength and carapace size in non-adult and adult male snow crab (*Chionoecetes opilio*). *J. Crust. Biol.* **20**, 399-406.

Gabriel, J. M. (1985). The development of the locust jumping mechanism. I. Allometric growth and its effect on jumping performance. *J. Exp. Biol.* **118**, 313-326.

Hafemann, D. R. and Hubbard, J. I. (1969). On the rapid running of ghost crabs (*Ocypode ceratophthalma*). *J. of Exp. Zool. A* **170**, 25-31.

Hahn, K. and LaBarbera, M. (1993). Failure of limb segments in the blue crab, *Callinectes sapidus* (Crustacea: Malacostraca). *Comp. Biochem. Physiol. A* **105**, 735-739.

Haley, S. R. (1969). Relative growth and sexual maturity of the Texas ghost crab, *Ocypode quadrata* (Fabr.) (Brachyura, Ocypodidae). *Crustaceana* **17**, 285-297.

Haley, S. (1973). On the use of morphometric data as a guide to reproductive maturity in the ghost crab, *Ocypode ceratophthalmus* (Pallas) (Brachyura, Ocypodidae). *Pac. Sci.* **27**, 350-362.

Hamasaki, K., Ishiyama, N., Yamashita, S. and Kitada, S. (2014). Survival and growth of juveniles of the coconut crab *Birgus latro* under laboratory conditions: implications for mass production of juveniles. *J. Crust. Biol.* **34**, 309-318.

Hartnoll, R. G. (1974). Variation in growth pattern between some secondary sexual characters in crabs (Decapoda Brachyura). *Crustaceana* **27**, 131-136.

Hartnoll, R. G. (1978). The determination of relative growth in Crustacea. *Crustaceana* **34**, 281-293.

Hartnoll, R. G. (1982). Growth. In *The Biology of Crustacea*, Vol. 2 (ed. L. G. Abele), pp. 111-196. New York: Academic Press.

Hartnoll, R. G. (1988). Evolution, systematics, and geographical distribution. In *Biology of the Land Crabs* (ed. W. W. Burggren and B. R. McMahon), pp. 6-54. Cambridge: Cambridge University Press.

Herreid, C. F. (1967). Skeletal measurements and growth of the land crab, *Cardisoma guanhumi* Latreille 1. *Crustaceana* **13**, 39-44.

Huxley, J. S. (1931). Notes on differential growth. *Am. Nat.* **65**, 289-315.

Huxley, J. S. (1972). *Problems of Relative Growth*. New York: Dover.

Ismail, S. Z. M. and Mykles, D. L. (1987). Differential atrophy in the dimorphic claws of male *Uca*. *Am. Zool.* **27**, 81A.

Jones, H. D. (1978). Fluid skeletons in aquatic and terrestrial animals. In *Comparative Physiology: Water, Ions and Fluid Mechanics* (ed. K. Schmidt-Nielsen, L. Bolis and S. H. P. Maddrell), pp. 267-281. Cambridge: Cambridge University Press.

Katz, S. L. and Gosline, J. M. (1992). Ontogenetic scaling and mechanical behaviour of the tibiae of the African desert locust (*Schistocerca gregaria*). *J. Exp. Biol.* **168**, 125-150.

Katz, S. and Gosline, J. (1994). Scaling modulus as a degree of freedom in the design of locust legs. *J. Exp. Biol.* **187**, 207-223.

Kelly, D. A. (2007). Penises as variable-volume hydrostatic skeletons. *Ann. N. Y. Acad. Sci.* **1101**, 453-463.

Kennedy, C. H. (1927). The exoskeleton as a factor in limiting and directing the evolution of insects. *J. Morph. Physiol.* **44**, 267-312.

Keudel, M. and Schrader, S. (1999). Axial and radial pressure exerted by earthworms of different ecological groups. *Biol. Fertil. Soils* **29**, 262-269.

Kier, W. M. (2012). The diversity of hydrostatic skeletons. *J. Exp. Biol.* **215**, 1247-1257.

Koehl, M., Quillin, K. J. and Pell, C. A. (2000). Mechanical design of fiber-wound hydraulic skeletons: the stiffening and straightening of embryonic notochords. *Am. Zool.* **40**, 28-041.

Krishnan, G. (1951). Phenolic tanning and pigmentation of the cuticle in Carcinus maenas. *J. Cell Sci.* **3**, 333-342.

Kurth, J. A. and Kier, W. M. (2014). Scaling of the hydrostatic skeleton in the earthworm *Lumbricus terrestris*. *J. Exp. Biol.* **217**, 1860-1867.

Kurth, J. A. and Kier, W. M. (2015). Differences in scaling and morphology between lumbricid earthworm ecotypes. *J. Exp. Biol.* **218**, 2970-2978.

Lin, H.-T., Slate, D. J., Paetsch, C. R., Dorfmann, A. L. and Trimmer, B. A. (2011). Scaling of caterpillar body properties and its biomechanical implications for the use of a hydrostatic skeleton. *J. Exp. Biol.* **214**, 1194-1204.

Lochhead, J. H. (1961). Locomotion. In *Physiology of Crustacea*, Vol. II (ed. T. H. Waterman), pp. 313-364. New York: Academic Press.

Lovett, D. L. and Felder, D. L. (1989). Application of regression techniques to studies of relative growth in crustaceans. *J. Crust. Biol.* **9**, 529-539.

Martinez, M. M. (2001). Running in the surf: hydrodynamics of the shore crab *Grapsus tenuicrustatus*. *J. Exp. Biol.* **204**, 3097-3112.

Martinez, M. M., Full, R. J. and Koehl, M. M. (1998). Underwater punting by an intertidal crab: a novel gate revealed by the kinematics of pedestrian locmotion in air *verus* water. *J. Exp. Biol.* **201**, 2609-2623.

McArdle, B. H. (1988). The structural relationship: regression in biology. *Can. J. Zool.* **66**, 2329-2339.

Mykles, D. L. and Skinner, D. M. (1982). Crustacean muscles: atrophy and regeneration during molting. In *Basic Biology Of Muscles: A Comparative Approach* (ed. B. M. Twarog, R. J. C. Levine and M. M. Dewey), pp. 337-357. New York: Raven Press.

Mykles, D. L. and Skinner, D. M. (1990). Atrophy of crustacean somatic muscle and the proteinases that do the job. A review. *J. Crust. Biol.* **10**, 577-594.

Otwell, W. S. (1980). *Harvest and Identification of Peeler Crabs*. University of Florida, Sea Grant Publication Number MAFS-26.

Parle, E., Herbaj, S., Sheils, F., Larmon, H. and Taylor, D. (2015). Buckling failures in insect exoskeletons. *Bioinspir. Biomim.* **11**, 016003.

Prange, H. D. (1977). The scaling and mechanics of arthropod exoskeletons. In *Scale Effects in Animal Locomotion* (ed. T. J. Pedley), pp. 169-181. Academic Press.

Queathem, E. (1991). The ontogeny of grasshopper jumping performance. *J. Insect Physiol.* **37**, 129-138.

Quillin, K. J. (1998). Ontogenetic scaling of hydrostatic skeletons: geometric, static stress and dynamic stress scaling of the earthworm *Lumbricus terrestris*. *J. Exp. Biol.* **201**, 1871-1883.

Quillin, K. J. (1999). Kinematic scaling of locomotion by hydrostatic animals: ontogeny of peristaltic crawling by the earthworm *Lumbricus terrestris*. *J. Exp. Biol.* **202**, 661-674.

Quillin, K. J. (2000). Ontogenetic scaling of burrowing forces in the earthworm *Lumbricus terrestris*. *J. Exp. Biol.* **203**, 2757-2770.

Raven, J. A. (1985). Comparative physiology of plant and arthropod land adaptation. *Philos. Trans. Royal Soc. London B* **309**, 273-288.

Rayner, J. M. V. (1985). Linear relations in biomechanics: the statistics of scaling functions. *J. Zool. Lond.* **206**, 415-439.

Roark, R. J. and Young, W. C. (1975). *Formulas for Stress and Strain*. New York: McGraw-Hill.

Sandon, H. (1937). Differential Growth in the crab *Ocypoda*. *J. Zool.* **107**, 397-414.

Schmidt-Nielsen, K. (1984). *Scaling: Why is Animal Size so Important?*. Cambridge University Press.

Skinner, D. M. and Graham, D. E. (1972). Loss of limbs as a stimulus to ecdysis in Brachyura (True crabs). *Biol. Bull.* **143**, 222-233.

Swartz, S. M. and Biewener, A. A. (1992). Shape and scaling. In *Biomechanics – Structures and Systems. A Practical Approach* (ed. A. A. Biewener), pp. 21-43. New York: Oxford Univ. Press.

Taylor, D. and Dirks, J.-H. (2012). Shape optimization in exoskeletons and endoskeletons: a biomechanics analysis. *J. R. Soc. Interface* **9**, 3480-3489.

Taylor, J. R. A. and Kier, W. M. (2003). Switching skeletons: hydrostatic support in molting crabs. *Science* **301**, 209-210.

Taylor, J. R. A. and Kier, W. M. (2006). A pneumo-hydrostatic skeleton in land crabs. *Nature* **440**, 1005.

Taylor, C. R., Schmidt-Nielsen, K. and Raab, J. L. (1970). Scaling of energetic cost of running to body size in mammals. *Am. J. Physiol.* **219**, 1104-1107.

Taylor, J. R. A., Hebrank, J. and Kier, W. M. (2007). Mechanical properties of the rigid and hydrostatic skeletons of molting blue crabs, *Callinectes sapidus* Rathbun. *J. Exp. Biol.* **210**, 4272-4278.

Teissier, G. (1960). Relative growth. In *Metabolism and Growth* (ed. T. H. Waterman), pp. 537-560. Academic Press.

Travis, D. F. (1955). The molting cycle of the spiny lobster, *Panulirus argus* Latreille. II. Pre-ecdysial histological and histochemical changes in the hepatopancreas and integumental tissues. *Biol. Bull.* **108**, 88-112.

Van Praagh, B. (1992). The biology and conservation of the giant Gippsland earthworm *Megascolides australis* McCoy, 1878. *Soil Biol. Biochem.* **24**, 1363-1367.

Wainwright, S. A. (1982). Structural systems: hydrostats and frameworks. In *A Companion to Animal Physiology* (ed. C. R. Taylor, K. Johansen and L. Bolis), pp. 325-338. New York: Cambridge University Press.

Wainwright, S. A., Biggs, W. D., Currey, J. D. and Gosline, J. M. (1976). *Mechanical Design in Organisms*. Princeton, NJ: Princeton Univ. Press.

Williams, D. L., Modla, S., Roer, R. D. and Dillaman, R. M. (2009). Post-ecdysial change in the permeability of the exoskeleton of the blue crab, *Callinectes sapidus*. *J. Crust. Biol.* **29**, 550-555.